The fractal structure in the ionization dynamics of Rydberg lithium atoms in a static electric field*

Deng Shan-Hong(邓善红), Gao Song(高 嵩), Li Yong-Ping(李永平),
Xu Xue-You(徐学友), and Lin Sheng-Lu(林圣路)†

College of Physics and Electronics, Shandong Normal University, Jinan 250014*, China*

(Received 1 July 2009; revised manuscript received 12 October 2009)

The ionization rate of Rydberg lithium atoms in a static electric field is examined within semiclassical theory which involves scattering effects off the core. By semiclassical analysis, this ionization process can be considered as the promoted valence electrons escaping through the Stark saddle point into the ionization channels. The resulting escape spectrum of the ejected electrons demonstrates a remarkable irregular electron pulse train in time-dependence and a complicated nesting structure with respect to the initial launching angles. Based on the Poincaré map and homoclinic tangle approach, the chaotic behaviour along with its corresponding fractal self-similar structure of the ionization spectra are analysed in detail. Our work is significant for understanding the quantum-classical correspondence.

Keywords: fractal structure, Poincaré map, homoclinic tangle, ionization of Rydberg atoms

PACC: 0555, 0545, 3280D

1. Introduction

Chaotic transport and escape of classical trajectories from a defined region of phase space have been of central concern for many years. However, there had been little relevant research on the atomic-scale until a well-known experimental development in 1996, where Lankhuijizen and Noordam experimentally studied the ionization rate of rubidium atoms excited by a weak short laser pulse in a constant applied electric field.[1,2] It was found that the ionization signal showed a train of electron pulses, rather than an exponential decay as previously expected. This observation had been qualitatively explained by the semiclassical analysis.[3] Nevertheless, the classical origin of the complication exhibited in the system is still obscure. Until very recently, motivated by this experiment, Mitchell *et al.* performed classical calculations to investigate ionization of hydrogen atoms in parallel electric and magnetic fields and reproduced a similar train of pulse in the ionizing spectrum.[4] Simultaneously, a fractal self-similar structure was obtained in the escape-time distribution versus electron launching angles. By using an area-preserving map in two-dimensional (2D) phase plane they associated the fractal structure with the escape dynamics of the ionized electrons. The map exhibits a homoclinic tangle, a hallmark of chaotic dynamics that is the typical mechanism for transporting and escaping processes. In a similar framework, Hansen[5] discussed the escape of particles from a vase-shaped cavity and Mitchell[6] explored the escape dynamics of ultra-cold atoms from an optical dipole trap which were explained by the recently developed symbolic dynamics. Both of the systems exhibit a prominent homoclinic tangle, and the fractal structure displayed in the escape-time versus launching angle distribution of the trajectories can always be attributed to the tangle.

It is well known that the ionization of hydrogen atoms in parallel electric and magnetic fields bears a certain chaotic behaviour owing to the magnetic field. Recent research showed that ionization of non-hydrogen atoms in an electric field or combined parallel electric and magnetic fields also gives rise to chaotic behaviours. From a quantum-mechanical point of view, it can be attributed to the core scattering effects.[7−9] However, significant challenges remain, especially for explaining the chaotic origin of the non-hydrogen atoms in constant external fields. As an example, we are concerned with the ionization of a lithium atom in an electric field in this paper. Based on the semiclassical theory, the so-called escape-time plot is theoretically computed to obtain the dependence of ionization rate on the escape time and the launching angle distribution, which provide a temporal and spatial resolution spectrum with fractal self-

*Project supported by the National Natural Science Foundation of China (Grant Nos. 10774093 and 10374061).
†Corresponding author. E-mail: sllin@sdnu.edu.cn
© 2010 Chinese Physical Society and IOP Publishing Ltd

similar structure. By means of the Poincaré map, the problem is reduced to a 2D phase plane where there exists a prominent homoclinic tangle induced by the transverse intersection of the stable and unstable manifolds arising from the hyperbolic fixed point. We predict that it is the infinitely repeated transverse intersections of the stable manifold with the line of initial condition that leads to the "fractal" structure in the escape-time plot. Thus a direct connection between the ionization spectrum in general geometric space and the homoclinic tangle in phase space is found. It allows us to analyse the self-similar fractal structure of the spectrum in detail.

This paper is organized as follows: Section 2 gives the Hamiltonian of the lithium atom in an electric field and explains the ionization process, connecting each peak of electron pulse to an ionization segment (icicle). Section 3 presents a 2D Poincaré map of the system and analyses the connection between the ionization spectra in general configuration space and the heteroclinic tangle in phase space. The relevant properties of the homoclinic tangle dynamics are described in Section 4. Section 5 illustrates the fractal self-similar features of the escape-time plot. Our conclusions are presented in the last section.

2. Hamiltonian and explanation of the ionization process

For studying the ionization process of the excited Rydberg atoms, the classical mechanics is indubitably important. The classical Hamiltonian of lithium atoms placed in an applied static electric field with cylindrical coordinates (ρ, z) and atomic units $(e \equiv \hbar \equiv m \equiv 1)$ is given by

$$H = \frac{1}{2}\left(P_z^2 + P_\rho^2\right) + V(\rho, z) + Fz, \tag{1}$$

where F is the electric field strength and the model potential $V(\rho, z)$ has the explicit form

$$\begin{aligned} V(\rho, z) &= V_{\text{Coulomb}}(\rho, z) + V_{\text{core}}(\rho, z) \\ &= -\frac{1}{\left(\rho^2 + z^2\right)^{1/2}} - \frac{Z-1}{\left(\rho^2 + z^2\right)^{1/2}} \left(1 + \frac{\left(\rho^2 + z^2\right)^{1/2}}{a}\right) \left\{\exp\left[\frac{-\left(\rho^2 + z^2\right)^{1/2}}{a}\right]\right\} \end{aligned} \tag{2}$$

with Z being the atomic number and a the parameter of the model potential that is chosen to give the measured quantum defect. For the case of lithium $Z = 3$, the optimised value of the parameter is given by $a = 1/2.13$.[10]

To gain a correspondence between the quantum and classical dynamics and eliminate the dependence of the dynamics on F, we introduce scaled variables.[11,12] Strictly speaking, when dealing with lithium atoms in an electric field, the scaling law no longer holds due to the model potential which decays exponentially and does not depend on the strength of the electric field within a few Bohr radius from the nucleus, hence could not be scaled by $F^{1/2}$. However, for the element with principal quantum number $N = 80$ in highly-excited states, the striking interaction region of the atomic core and the valence electron is relatively small, and in semiclassical analysis, it allows the ignoring of the core-induced effects and consideration of only the effects of the pure Coulomb force combined with the external field outside the region. Since only the long-distance orbits are important for calculation of the ionization rate, thus on ignoring the small region around the core, the scaling law remains a reasonable approximation.

For $\tilde{r} = rF^{1/2}$, $\tilde{P} = PF^{-1/4}$, $\varepsilon = EF^{-1/2}$, $\tilde{t} = t'F^{3/4}$, the Hamiltonian becomes

$$\begin{aligned} \tilde{H} = \varepsilon = \frac{1}{2}\left(\tilde{P}_\rho^2 + \tilde{P}_z^2\right) &- \frac{1}{\left(\tilde{\rho}^2 + \tilde{z}^2\right)^{1/2}} \\ &- \frac{Z-1}{\left(\tilde{\rho}^2 + \tilde{z}^2\right)^{1/2}} \left(1 + \frac{\left(\tilde{\rho}^2 + \tilde{z}^2\right)^{1/2}}{a}\right) \\ &\times \left\{\exp\left[\frac{-\left(\tilde{\rho}^2 + \tilde{z}^2\right)^{1/2}}{a}\right]\right\} + \tilde{z}. \end{aligned} \tag{3}$$

In order to eliminate the singularity induced by the Coulomb term in the Hamiltonian, the parabolic coordinates (u, v) are adopted

$$u = (\tilde{r} + \tilde{z})^{1/2}, \quad v = (\tilde{r} - \tilde{z})^{1/2}, \tag{4}$$

$$p_u = \tilde{p}_\rho v + \tilde{p}_z u, \quad p_v = \tilde{p}_\rho u - \tilde{p}_z v,$$

$$\mathrm{d}t = (u^2 + v^2)\mathrm{d}\tilde{t}, \tag{5}$$

where $\tilde{t}$ is the scaled time and its scaled unit equals 52 picoseconds in a static electric field of 19 V/cm. By introducing an effective Hamiltonian, $h = 2\tilde{r}(\tilde{H} - \varepsilon)$ we have

$$h(u, v, p_u, p_v) = \frac{1}{2}(p_u^2 + p_v^2) + V(u, v) - 2, \quad (6)$$

$$V_{uv} = -\varepsilon(u^2 + v^2) + \frac{1}{2}(u^4 - v^4) - 4\left\{\exp\left[\frac{-(u^2 + v^2)}{2a}\right]\right\}, \quad (7)$$

which is the Hamiltonian used in this paper.

The lithium atoms in a constant electric field are excited by a short laser pulse. Considering the defined bandwidth of the laser pulse, a coherent superposition of several Stark states is excited, creating an outgoing radial wave packet in all directions, which consists of the initial outgoing Coulomb wave as can be computed using the semiclassical method developed in Ref. [13]. According to the extended-closed orbit theory, the outgoing wave packet can be modelled by an ensemble of classical trajectories travelling away from the nucleus in all directions, which is well described by

$$\Phi_0(r_0, \theta_i^j) = -\mathrm{i}\,\pi^{1/2} 2^{3/4} r_0^{-3/4} \times \mathrm{e}^{\mathrm{i}(\sqrt{8r_0} - 3\pi/4)} y(\theta_i^j), \quad (8)$$

where $y(\theta)$ is the angular distribution. The angles θ are defined relative to the positive z-axis when considered in cylindrical coordinates. Some trajectories progress directly toward a detector and are accelerated by the external field, creating the prime pulse of electrons. The other trajectories, which initially deviate from the field direction, are turned around by the field and return to the vicinity of the core, where they are scattered by the core in all directions. The scattered trajectories, depending on their outgoing directions, may propagate directly toward the detector to produce a second pulse of electrons or be turned around again by the field and rescattered by the core. The ionized electron pulses with scaled energy at $\varepsilon = -1.3$ are shown in Fig. 1(a), in which the ionization rate is computed as a function of time an escaping trajectory spends before arriving at the detector.[7,8] Figure 1(b) displays the continuous-escape-time plot, i.e. the time that an escaping trajectory takes to strike the detector versus its initial launch angle. The plot exhibits an infinite number of icicle-like fragments, termed as icicles. Each icicle corresponds to a peak of pulse in the ionization-time plot. The two critical angles θ_c of each icicle imply that the trajectories with these launch angles will take infinite time to arrive at the detector. Trajectories with initial launch angles between the two critical angles will reach the detector and result in escape, thus each icicle corresponds to an escape segment. The structure of the icicles or the pulse train reveals a certain fractal structure known as epistrophe self-similarity.[14] The Poincaré map will be introduced in Section 3 for a detailed understanding of the classical escape dynamics.

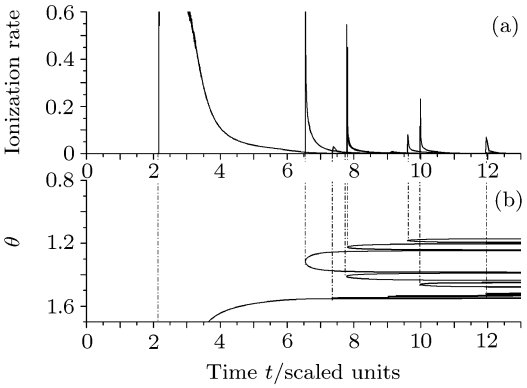


Fig. 1. (a) The ionization rate for Rydberg lithium atoms in a static electric field with $\varepsilon = -1.3$, $N = 80$, $F = 19$ V/cm. (b) The continuous-escape-time plot: the time it takes a trajectory to strike the detector ($z = -4$) is plotted as a function of its initial launch angle θ of the electron trajectories. The dashed line connects the direct ionization and the corresponding pulse in (a).

3. Poincaré map

We convert the continuous-time dynamics in the four-dimensional phase space (u, v, p_u, p_v) to a discrete-time Poincaré map on a 2D (v, p_v) surface of section by the constraints $u = h = 0$. The map is defined as

$$v_2 = v_1 + \frac{\partial G(\bar{v}, \bar{p}_v)}{\partial \bar{p}_v},$$
$$p_{v_2} = p_{v_1} - \frac{\partial G(\bar{v}, \bar{p}_v)}{\partial \bar{v}}, \quad (9)$$
$$\bar{v} = (v_1 + v_2)/2,$$
$$\bar{p}_v = (p_{v1} + p_{v2})/2, \quad (10)$$

where the "Poincaré generator"[15,16] $G(v, p_v)$ is

$$G(v, p_v) = \tau\left[\frac{p_v^2}{2} - \varepsilon v^2 - \frac{v^4}{2} - 4\exp\left(\frac{-v^2}{2a}\right)\right]. \quad (11)$$

We examine the Poincaré map at $\varepsilon = -1.3$. As in Fig. 2(a), this map possesses two unstable fixed points with a pair of stable (thick curve) and unstable (thin curve) manifolds attached to them. The positions of

the fixed points of the map are determined by solving Eqs. (9) with $v_2 = v_1$ and $p_{v_2} = p_{v_1}$. The unstable manifold of either fixed point can be calculated by iterating forward a distribution of points on the linearized manifold in the vicinity of the fixed point. Similarly, the stable manifold can be obtained by corresponding backward mappings. Because the fixed points are unstable and hyperbolic, a heteroclinic tangle is formed as in Fig. 2(a). Roughly speaking, the region confined by the manifolds corresponds to the bounded states of the trajectories. All trajectories with fixed energy ε start from the surface of section and at precise time $t = 0$. Thus, the initial condition line L_0 is parameterized by the initial outgoing angle θ according to $p_v = 3.464\sin(\theta/2)$, as derived from Eqs. (9) and (10), along with the fact that $p_u^2 + p_v^2 = 12$, at $u = v = 0$. The vertical line L_0 with $v = 0$ and p_v covering the region between ± 3.464 on the surface of section populates the initial conditions for the outgoing trajectories from the core in all directions with constant energy. We find a direct connection between the continuous-escape-time plots in general geometric space and the heteroclinic tangle manifolds in phase space.

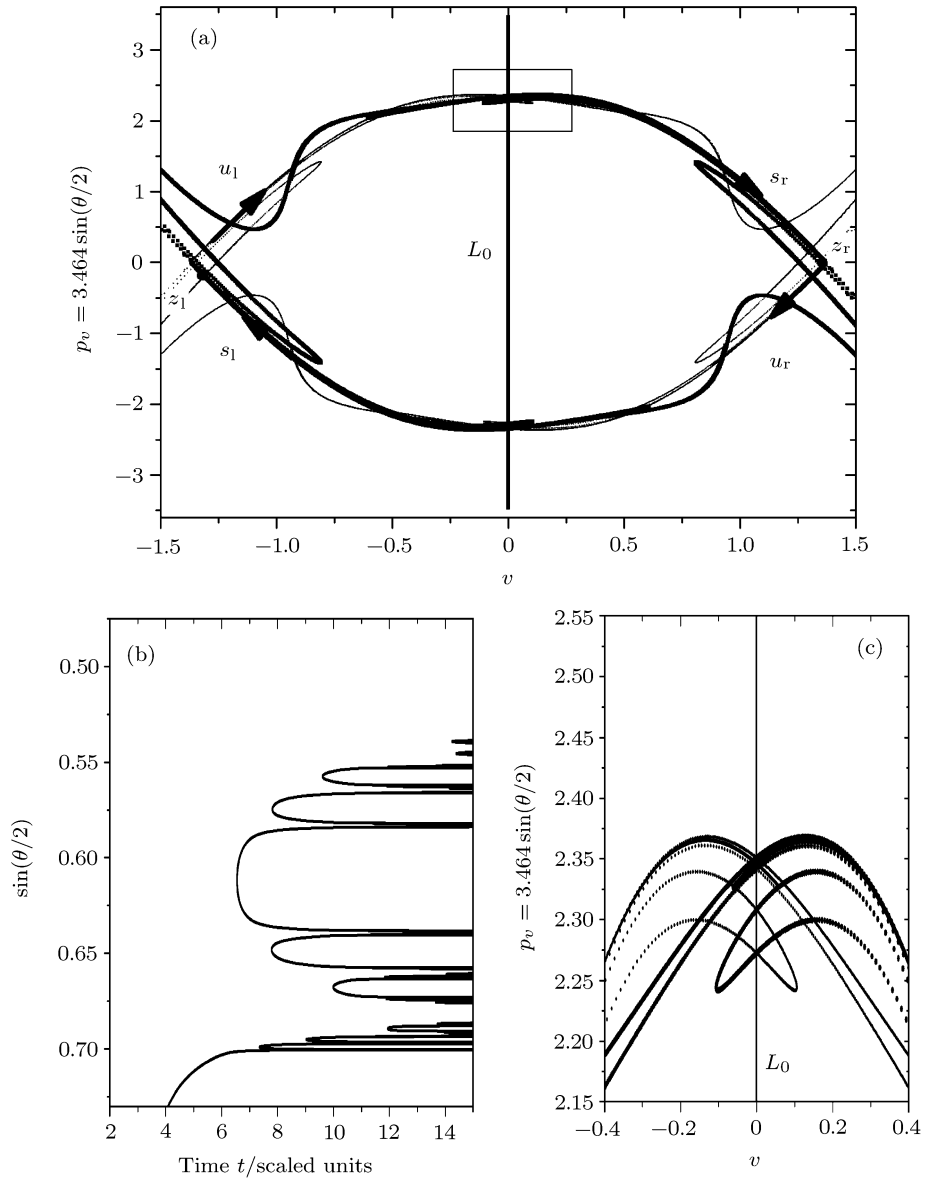


Fig. 2. (a) The surface of section plot for $\varepsilon = -1.3$ in the (u, v) coordinates, showing that the right stable manifold s_r (thick curve) and the left unstable manifold u_l (thin curve) intersect an infinite number of times. The same is true for s_l and u_r. (b) The corresponding continuous escape-time plot, in which $\sin(\theta/2)$ is plotted as a function of t. (c) The magnification of the rectangle inset in (a).

One can see from Figs. 2(b) and 2(c), for example, that a stable manifold originating from the fixed points will pass through the line L_0, with iteration, they will intersect many times. Each intersection between L_0 and the stable manifold $s_{\rm l}$ or $s_{\rm r}$ creates an edge of an icicle. Intervals formed on the line L_0 which result from its truncation by the stable manifold correspond to the escape segments. The infinity of such intersections results in the infinity of icicles.

4. The homoclinic tangle and phase space escape

Note that the surface-of-section plot is invariant under the transformation $(v, p_v) \to -(v, p_v)$, we can therefore convert the heteroclinic tangle to a homoclinic tangle by canonical transform. In terms of canonical polar coordinate $I = (P_v^2 + v^2)/2$ and $\phi = -\tan^{-1}(p_v/v)$, we define $p = -\sqrt{I}\sin 2\phi = \sqrt{2}vp_v(v^2 + p_v^2)^{-1/2}$ and $q = \sqrt{I}\cos 2\phi = (v^2 - p_v^2)[2(v^2 + p_v^2)]^{-1/2}$. Thus in the new coordinates, $+(v, p_v)$ and $-(v, p_v)$ are identified and the vertical line in Fig. 2(a) that populates initial conditions now becomes a horizontal one. The two unstable fixed points in Fig. 2(a) now become a single unstable fixed point z_x, meanwhile, the attached stable and unstable manifolds intersecting transversely incorporates the same dynamics, however, substantially simplified in tangle shape. Because both manifolds are invariant under iteration, once they intersect at a point, they will intersect at all their forward and backward iteration. If there is one homoclinic intersection, then there will be infinite homoclinic intersections, accompanying which is the stretching and folding of the manifolds, leading to a very complicated structure called a homoclinic tangle. According to the Smale–Birkhoff theorem, the existence of a homoclinic tangle is intrinsic evidence that the flow is chaotic.

As seen in Fig. 3, the stable and unstable manifolds have a prime intersection denoted by P_0, and the subscript 0 means it is the first intersection of the manifolds. The "complex" is the region bounded by the segments of the stable and unstable manifolds joining z_x to P_0. The points within the complex correspond to the neutral atoms. Escape is defined as mapping out of the complex. If a trajectory maps out of the complex, it will subsequently progress to infinity, resulting in the observed escape electron pulse.

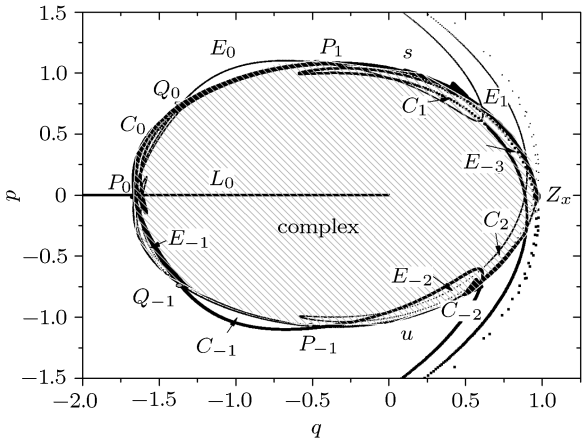


Fig. 3. The homoclinic tangle plot for $\varepsilon = -1.3$. $F = 19$ V/cm in the (q, p) coordinates, an unstable fixed point z_x is attached by stable manifold s (thick curve) and unstable manifold u (thin curve). The shaded region is "complex", points within the complex correspond to a neutral atom. C_k and E_k represent capture lobes and escape lobes.

Since P_0 is the first intersection of the stable and unstable manifolds, then there will be infinite intersections by its infinite forward and backward iteration, which can be denoted as P_1, $P_2, \ldots$ for forward iterations and P_{-1}, $P_{-2}, \ldots$ for backward iterations. The subscript of P marks the number of iterations. The positive sign denotes the forward iteration (which is omitted here) and the minus the backward. Obviously, these intersections remain on the manifold for large number of iterations, and will approach the fixed point z_x as the number of iterations tends to infinity. These intersections are called homoclinic points. The orbit formed by these intersections is called a homoclinic orbit and plays an important role in the global dynamics of the map. Since Poincaré map is orientation preserving, the homoclinic points may be separated by at least one further point, denoted as Q_k. That is to say, between P_0 and P_1, there exists another point Q_0. The segment of stable and unstable manifold between P_1 and Q_0 bound a prime lobe E_0 called escape lobe, where E means "escape", namely, points in the area formed by the lobe will finally escape the complex for certain positive iteration numbers. Points in E_0 (or lobe E_0) can be mapped backward to E_{-1}, $E_{-2}, \ldots$ and forward to E_1, $E_2, \ldots$ respectively. The prime lobe E_0 plays an important role in escape dynamics. It can be deemed as a "turnstile" which means all points in E_{-k} will escape from the complex when they enter E_0 by k-times mapping $E_0 = M^k(E_{-k})$. As these lobes are mapped backward, their widths are compressed and their lengths stretched. They become

long and thin and develop an intricate twisted shape. Thus when the escape lobes are long and thin enough to have intersections with the line of initial conditions L_0, these intersections (the escape segment) will escape the complex after certain number of iterations. For instance, each escape segment that escapes on the k-th iteration is an interval of intersection between the escape lobe E_{-k} and the line of initial conditions L_0. Accordingly, the segments of s and u between Q_0 and P_0 enclose the "capture" lobe C_0. Analogously, on one iteration of the map, all points in C_{-1} (outside the complex), will arrive in C_0, which is inside the complex indicating that it is captured.

We use a global topological quantity D to characterize the structure of the tangle.[4] It defines a minimum delay time denoted by the number of iterations any scattering trajectory may spend within the complex. In fact, the parameter D is the smallest n such that $E_{k-(n+1)}$ intersects C_k for arbitrary k. In Fig. 3, E_{-3} is the first escape lobe that intersects C_1, then it will be E_{-4}, $E_{-5}, \ldots$ (which are too narrow and thin in the plot to be seen noticeably), so 3 is the smallest n according to the above definition and thus we obtain $D = 3$ in the case.

5. Epistrophes and the fractal self-similarity

The Poincaré map converts a continuous-escape-time plot into a discrete-escape-time plot and on the surface of section the tangle of the map exhibits series of escape regions and capture regions as seen in Fig. 3. In chaotic theory, the fact that the unstable manifold folds an infinite number of times is precisely the reason why the "attractor" has a fractal structure. A spectrum is self-similar in the sense that a smaller piece of it can reproduce the entire spectrum upon magnification. For the spectrum of the ionization rate the chaotic property is indirectly reflected in the escape-time plot, particularly in the patterns of the escape segments (the "icicles"), yet characterizing the fractal requires a concrete analysis on the global topological structures, which can be achieved by analysing the structure of the tangle. Figure 4 shows three successively magnified intervals of initial launch-angle distributions of the ionized electrons which can be realized by improving spectral resolution in numerical calculations.

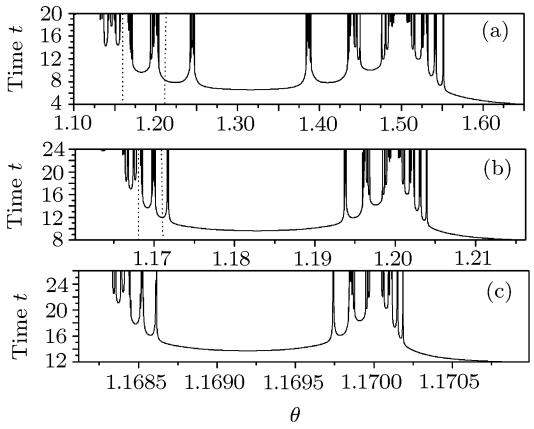


Fig. 4. The successive magnifications of the escape-time plot. (a) The escape-time plot with respect to electronic initial angles of lithium atoms at scaled energy $\varepsilon = -1.3$. The applied external electric field strength is $F = 19$ V/cm, and the time needed to take a trajectory to strike the detector is plotted as a function of the initial launched angles of escape electrons. (b) The plot of assigned angle interval by dashed line between 1.1602 and 1.2162 in figure (a) is magnified and, (c) the magnifications of the regions between 1.68121 and 1.17099 in figure (b).

We find that similar structure is replicated at higher and higher levels of magnifications, and occurs on all smaller scales so as to form a regular nesting structure. These regular sequences of the escape segments are called epistrophes as in Ref. [14]. The epistrophe fractal is a generalization of a kind of fractal in which at all levels of resolution there are variable beginnings and self-similar endings. In tangle dynamics they are characterized by a sequence of infinite number of consecutive escape segments converging to some point on the line of initial condition in phase space. Figure 5(b) shows the discrete escape-time plot, which shows how the number of iterations that the Poincaré map requires for the trajectory to escape the complex changes with the initial incident angle. Each escape segment corresponds to an icicle in Fig. 5(a), which connects the continuous escape-time plot in configuration space with the discrete Poincaré map in phase space. Every escape segment denoted in the plot belongs to a certain epistrophe except the direct segment. The number of iterations for the direct segment is zero, implying that trajectories with incident angles in the range will escape without any iteration. That is, the direct segment corresponds to trajectories without undergoing core-scattering effect. As for segment A_1, which belongs to epistrophe A with four as corresponding number of iteration, all trajectories with incident angles in this range will iterate four

times before escaping to cause ionization. Therefore, A_1 is formed by the intersection of the initial condition L_0 and the escape lobe E_{-4} (which is the first escape lobe long and thin enough to reach and overshoot L_0) in the Poincaré map. Similarly, A_2 is formed by the intersection of L_0 with E_{-5}, trajectories escaping the complex after five iterations. A_3, $A_4, \ldots$ are formed alike. Approaching the unstable fixed point, the escape lobes become thinner, so do the corresponding escape segments, which are bound to form since the lobes are then long enough to intersect L_0. Thus the escape segments will ultimately converge to a point on L_0. Considering epistrophe A in Fig. 5, it begins at $n = 4$ and converges upon the upper end point of the "direct" segment, and contains each subsequent segment at $n = 5$, $6 \ldots$ Similarly, epistrophes B and C occur on the fifth iteration and converge upon the upper and lower end points of A_1 respectively. As for why the epistrophes B and C start from $n = 5$, we have to refer to the "epistrophe start rule",[14] derived by Mitchell *et al.* Any escape segment on the n-th iteration produces two new epistrophes on iteration $k = n+D+1$, where the global topologic parameter D ($D = 3$) is a certain "minimal set" of escape segments in the homoclinic tangle. For example, the number of iteration for A_1 is four, then it will be eight for B and C, obtained by $4 + 3 + 1 = 8$. Similarly, A_2 with iteration number $n = 5$ will produce two new epistrophes with $n = 9$. However, not all the escape segments fit the "epistrophe start rule". We call them "strophe", which are marked by asterisks.[17] The "strophe" is still obscure to present knowledge, so it is beyond our discussion here.

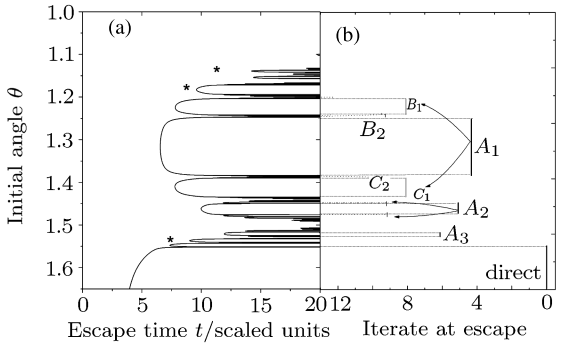


Fig. 5. (a) The continuous-escape time plot: the time needed to take a trajectory to strike the detector is plotted as a function of the initial launch angle θ. (b) The discrete-escape-time plot: the number of iterations of the Poincaré map required to escape the complex is plotted versus θ.

Since a homoclinic tangle in phase space is the cause of the epistrophe-fractal and self-similar structure in the escape-time plot and because each icicle in the escape-time plot has a one to one correspondence with the ionizing pulse in the ionization rate versus time plot as shown in Fig. 1, we can predict that the time evolution of the ionization rate also exhibits similar epistrophe-fractal structure. So the epistrophe exhibited in the escape-time plot is expected to exist in the ionizing spectrum in Fig. 1(a). Therefore the epistrophe exhibited in the fractal has significant importance in predicting when the ionizing pulses start and how they behave over the course of time.

6. Conclusions

Using the semiclassical method, we theoretically calculated the ionization rate and the escape-time plot of lithium atoms in a static electric field by integration of classical trajectories starting out from the core in all directions. Remarkable irregular electron pulse trains as well as the continuous-escape-time plot representing the dependence of the escape time on the initial launch angle of the trajectories were obtained. The continuous-escape-time plot in general geometric space exhibits numerous icicle-like structures that can be related to a homoclinic tangle in phase space by a Poincaré map, which can be converted to the discrete escape-time plot. The homoclinic tangle appearing in the system can generally be used to interpret phase space transport and escape. Furthermore, we have obtained the minimum iteration number D by analysing the homoclinic tangle of the map. In the magnified part of the escape-time plot, similar structure is visible, indicating that the fractal structure takes place on all scales. Since the peak of each pulse in the ionizing spectra corresponds well to the tip of each icicle in the escape-time plot, the analysis on the epistrophe-fractal contributes to understanding of the structure of the pulse trains. Because the pulse trains in the ionizing spectra are caused by the core-scattering effect from the quantum-mechanical point of view, while the escape-time plot and Poincaré map are obtained classically, our study has significant importance for the understanding of the quantum-classical correspondence. The investigation in this paper could also provide a convenient laboratory tool for studying chaotic transport and escape. Since the essential feature of chaotic dynamics lies in its sensitive dependence upon the initial conditions such as the initial launching angles, we expect this work can provide a reliable probe to measure the model potential of multi-electron atoms.

References

[1] Lankhuijzen G M and Noordam L D 1995 *Phys. Rev.* A **52** 2016

[2] Lankhuijzen G M and Noordam L D 1996 *Phys. Rev. Lett.* **76** 1748

[3] Robicheaux F and Shaw J 1996 *Phys. Rev. Lett.* **77** 4154
Robicheaux F and Shaw J 1997 *Phys. Rev.* A **56** 278

[4] Mitchell K A, Handley J P, Tighe B and Delos J B 2004 *Phys. Rev. Lett.* **92** 073001
Mitchell K A, Handley J P, Tighe B and Delos J B 2004 *Phys. Rev.* A **70** 043407

[5] Hansen P, Mitchell K A and Delos J B 2006 *Phys. Rev.* E **73** 066226

[6] Mitchell K A and Steck D A 2007 *Phys. Rev.* A **70** 031403

[7] Zhou H, Li H Y, Gao S, Zhang Y H, Jia Z M and Lin S L 2008 *Chin. Phys.* B **17** 4428

[8] Lin S L, Zhou H, Xu X Y, Jia Z M and Deng S H 2008 *Chin. Phys. Lett.* **25** 4251

[9] Gao S, Xu X Y, Zhou H, Zhang Y H and Lin S L 2009 *Acta Phys. Sin.* **58** 1473 (in Chinese)

[10] Courtney M, Spellmeyer N, Jiao H and Kleppner D 1995 *Phys. Rev.* A **51** 3604

[11] Gao J, Delos J B and Baruch M 1992 *Phys. Rev.* A **46** 1449

[12] Haggerty M R and Delos J B 2000 *Phys. Rev.* A **61** 053406

[13] Dando P A, Monteiro T S, Delande D and Taylor K T 1996 *Phys. Rev.* A **54** 127

[14] Mitchell K A, Handley J P, Tighe B and Delos J B 2003 *Chaos* **13** 880
Mitchell K A, Handley J P, Tighe B and Delos J B 2003 *Chaos* **13** 892

[15] Meyer K R 1970 *Trans. Am. Math. Soc.* **149** 95

[16] Meyer K R and Hall G R 1992 *Introduction to Hamiltonian Dynamical Systems and the N-Body Problem* (New York: Springer) p. 224

[17] Courtney M, Spellmeyer N, Jiao H and Kleppner D 1995 *Phys. Rev.* A **51** 3604